HHS Public Access

Author manuscript

Sci Transl Med. Author manuscript; available in PMC 2016 June 10.

Published in final edited form as:

Sci Transl Med. 2015 June 10; 7(291): 291ra97. doi:10.1126/scitranslmed.aaa5370.

Basal exon skipping and genetic pleiotropy: A predictive model of disease pathogenesis

Theodore G. Drivas[1,*], **Adam P. Wojno**[1,*], **Budd A. Tucker**[2], **Edwin M. Stone**[2,3], and **Jean Bennett**[1,†]

[1]Center for Advanced Retinal and Ocular Therapeutics, F. M. Kirby Center for Molecular Ophthalmology, Perelman School of Medicine, University of Pennsylvania, Philadelphia, PA 19104, USA

[2]Stephen A. Wynn Institute for Vision Research, University of Iowa, Iowa City, IA 50309, USA

[3]Howard Hughes Medical Institute, Department of Ophthalmology and Visual Sciences, University of Iowa Carver College of Medicine, Iowa City, IA 50309, USA

Abstract

Genetic pleiotropy, the phenomenon by which mutations in the same gene result in markedly different disease phenotypes, has proven difficult to explain with traditional models of disease pathogenesis. We have developed a model of pleiotropic disease that explains, through the process of basal exon skipping, how different mutations in the same gene can differentially affect protein production, with the total amount of protein produced correlating with disease severity. Mutations in the *centrosomal protein of 290 kDa* (*CEP290*) gene are associated with a spectrum of phenotypically distinct human diseases (the ciliopathies). Molecular biologic examination of *CEP290* transcript and protein expression in cells from patients carrying *CEP290* mutations, measured by quantitative polymerase chain reaction and Western blotting, correlated with disease severity and corroborated our model. We show that basal exon skipping may be the mechanism underlying the disease pleiotropy caused by *CEP290* mutations. Applying our model to a different disease gene, *CC2D2A* (*coiled-coil and C2 domains–containing protein 2A*), we found that the

†Corresponding author. jebennet@mail.med.upenn.edu.
*These authors contributed equally to this work.

Author contributions: T.G.D. and A.P.W. conceived of, designed, and performed all experiments and wrote the paper. E.S., B.T., and J.B. helped in the acquisition of samples and clinical data, designing of experiments, and editing of the manuscript.

Competing interests: J.B. is a co-inventor of a patent for a method to treat or slow the development of blindness but waived any financial interest in this technology in 2002. J.B. and T.G.D. are co-inventors on a U.S. provisional patent 61847,016, peripherally related to the subject of this study, “Gene Therapy for Disorders Related to CEP290.” J.B. serves on scientific advisory boards for Avalanche Technology, Spark Therapeutics, and Sanofi-Aventis, is a consultant for Novartis, and is a founder of GenSight Biologics. The other authors declare that they have no competing interests.

Data and materials availability: Reagents and cell lines are available subject to current U.S. regulations relating to human subject studies.

SUPPLEMENTARY MATERIALS

www.sciencetranslationalmedicine.org/cgi/content/full/7/291/291ra97/DC1

Fig. S1. Human *CEP290* mutations classified on the basis of their predicted coding effects.
Fig. S2. Levels of *CEP290* transcript lacking certain exons, normalized to total CEP290 levels.
Table S1. Phenotypes of *CEP290* disease.
Table S2. Mutations harbored by reported *CEP290* patients.
Table S3. Mutations harbored by reported *CC2D2A* patients.
Table S4. Tabular presentation of data.

same correlations held true. Our model explains the phenotypic diversity of two different inherited ciliopathies and may establish a new model for the pathogenesis of other pleiotropic human diseases.

INTRODUCTION

Genetic pleiotropy, the phenomenon through which mutations in the same gene can result in markedly different disease phenotypes, has proven difficult to explain using traditional models of disease pathogenesis (1). Pleiotropy seems to mandate that different mutations affect protein function differently, but for many genes, no relationship has been established between specific mutations and distinct functional outcomes. Perhaps the origin of pleiotropy lies not in the effects of particular mutations on protein function but rather in the effects of particular mutations on total expression of functional protein.

There is evidence to suggest that detrimentally mutated exons that begin and end in the same reading frame can be selectively excluded from the final gene transcript through a process known as nonsense-associated alternative splicing (Fig. 1A) (2–5). The resultant low expression of minimally shortened, but otherwise intact, transcripts might produce meaningful amounts of near-full-length protein that retains some or all of the full-length protein's functionality. Thus, for a given gene, different classes of mutations in different exons might be predicted to result in different degrees of full-length and near-full-length proteins, with total expression of functional protein correlating with and explaining the different phenotypes of pleiotropic diseases.

Such exon skipping mediated by nonsense-associated alternative splicing has recently been demonstrated in the *centrosomal protein of 290 kDa* (*CEP290*) gene (6), mutations in which are associated with a spectrum of devastating and phenotypically distinct human disease syndromes (table S1) (7, 8). The least severe *CEP290*-associated phenotype is Leber congenital amaurosis (LCA), characterized by retinal dystrophy with no extraocular symptoms. More moderate *CEP290*-associated symptoms include Senior-Løken syndrome (SLS), characterized by both retinal and renal abnormalities, and Joubert syndrome (JS) and Joubert syndrome–related disorders (JSRDs). JS is defined by abnormalities in the central nervous system (CNS) including under-development of the cerebellar vermis and brain stem and decreased muscle tone, whereas JSRD is defined as JS with additional extra-CNS manifestations (kidney disease and/or LCA). Unlike other ciliopathy disease genes, more than 95% of patients with *CEP290* mutations who show signs of JS are ultimately found to have renal and retinal diseases (table S2), highlighting how mutations in this gene truly cause a spectrum of disease, rather than a number of distinct disease states. Finally, in the most severe cases, *CEP290* mutations are associated with the Meckel-Gruber syndrome (MKS) and Meckel-like syndrome (ML), both characterized by lethality due to severe, multiorgan involvement. The pathology observed in all of these syndromes is due to CEP290's essential role in the development and maintenance of the primary cilium (9, 10), a cellular organelle critical in cell signaling and development (11–13). As a pleiotropic disease gene that is subject to nonsense-associated alternative splicing–mediated exon skipping,

CEP290 seemed an ideal candidate to test our theory that total functional protein might explain the pleiotropy observed in certain diseases.

RESULTS

To formulate and assess our model, we first classified all 138 known human *CEP290* mutations (14–19) on the basis of their predicted coding effects (fig. S1). Mutations were divided into three categories—mild, moderate, and severe—on the basis of the amount of full-length and near-full-length CEP290 proteins that we predicted each mutant transcript would produce. Mild mutations were those that were predicted to have only small effects on total amounts of CEP290 protein. These included all known *CEP290* missense mutations and the common intron 26 c.1655A>G mutation, which has been reported to result in only a 50% reduction in normal *CEP290* transcript (20). All truncating mutations, on the other hand, were classified as either moderate or severe. Moderate mutations were those that produced a premature stop codon within an exon beginning and ending in the same reading frame. Transcripts including the mutated exon and premature stop codon would be expected to undergo nonsense-mediated decay (21, 22) and result in little or no full-length or near-full-length CEP290 protein, whereas those transcripts skipping the mutated exon, through the process of nonsense-associated alternative splicing, should result in the production of low levels of near-full-length CEP290 protein (Fig. 1A, I and II). Conversely, severe mutations were those that produced a premature stop codon within an exon beginning and ending in different reading frames. Thus, transcripts either including or skipping the mutated exon (resulting in a frameshift) should both be subject to nonsense-mediated decay, resulting in no production of full-length or near-full-length CEP290 protein (Fig. 1A, III and IV).

Using this classification system, we established a model for the prediction of total full-length or near-full-length CEP290 protein for any patient with known homozygous or compound heterozygous *CEP290* disease alleles (Fig. 1B). Hypothesizing that the predicted protein amounts might correlate with different *CEP290* disease phenotypes, we categorized different phenotypes according to predicted total protein as part of our model. Applying our model to all 250 *CEP290* patients described in the literature (table S2) (14–19), a striking correlation was immediately apparent—predicted protein amounts were significantly associated with disease severity ($P < 0.0001$, Fisher's exact test) (Fig. 2A). Ninety percent of patients with LCA, the least severe of the *CEP290* phenotypes, were predicted to have high to medium amounts of CEP290 protein. Predicted CEP290 amounts in patients with moderate disease (SLS and JS/JSRD) were more evenly distributed across different predicted protein amounts. Finally, 100% of patients with ML and MKS, the most severe of the *CEP290* phenotypes, were predicted to have low to absent CEP290 (Fig. 2A).

Whereas predicted protein amounts correlated with the severity of *CEP290* disease, 32 patients presented with phenotypes that were more severe than predicted by our model. Examining the mutations harbored by these patients, a pattern quickly became clear. More than 70% ($n = 23$) of these patients were found to harbor truncating mutations within exon 6, 9, 40, or 41. Although each of these mutations was considered only moderate by our model, each of these patients presented with very severe disease.

A potential explanation for the deleterious nature of these particular mutations became apparent when we mapped them to domains of CEP290 known to play critical roles in the interactions of this protein. Exons 6 through 9 lie at the center of CEP290's recently described membrane association domain, whereas exons 40 and 41 make up the core of CEP290's critical microtubule-binding domain (Fig. 2B) (10). Splice variants lacking any of these four exons might escape nonsense-mediated decay and produce low amounts of near-full-length CEP290, all of which, however, would lack regions critical to the protein's function. It is interesting to note that most of patients with MKS or ML were found to harbor mutations in these particular exons, suggesting that patients expressing very low amounts of CEP290 lacking critical functional regions fare worse than those expressing no CEP290 at all.

Taking the critical nature of exons 6, 9, 40, and 41 into account, we modified our model to predict levels of full-length and near-full-length CEP290 with intact microtubule- and membrane-binding domains, rather than absolute levels of CEP290. Application of this model to all of the *CEP290* patients described in the literature (table S2) (14–19) again showed that predicted protein levels were robustly associated with disease severity ($P < 0.0001$, Fisher's exact test) (Fig. 2C).

To more rigorously interrogate our model, we assembled a small cohort of unreported *CEP290* patients with diverse genotypes and symptoms. These patients and their medical records were carefully examined and summarized by a single clinician masked to the patients' genotypes (Fig. 3A). We applied our model to each of these patients and saw that, again, predicted CEP290 protein accurately correlated with patient phenotype. All patients predicted to have high to medium levels of CEP290 were diagnosed only with LCA, whereas patient 582, predicted to have very low CEP290 protein, carried a diagnosis of Joubert syndrome with retinal dystrophy.

This small but well-characterized cohort of patients revealed an even finer correlation between predicted protein amounts and patient phenotypes. Patient 54, predicted to have high levels of CEP290, was found to have a Snellen visual acuity of 20/80, by far the best of the patients examined. Similarly, patients 62, 619, and 620, all predicted to have medium levels of CEP290, with one mild and one moderate allele, were found to have at least some residual light perception despite having advanced retinal degeneration. On the other hand, patients 294 and 182, both predicted to have medium amounts of CEP290 protein, but with one mild and one severe allele, were found to have no residual light perception (Fig. 3A).

To confirm that the amount of protein predicted by our model correlates with CEP290 protein expression in patient tissue, we measured full-length and near-full-length CEP290 in primary dermal fibroblasts isolated from each of the patients in our cohort and from three normal healthy controls by Western blotting (Fig. 3, B and C). Strikingly, CEP290 protein robustly correlated with the amounts predicted by our model (Fig. 3C). Patient 54, predicted to have high protein levels, was found to have roughly 50% of normal CEP290. Those patients predicted to have medium protein levels were found to have roughly 33% of normal amounts of CEP290 protein. Patient 582, predicted by our model to have very low protein amounts, was found to have only 8.5% of normal CEP290. It should be noted that, in a

traditional model of cellular transcription and translation, patient 582, harboring truncating mutations in both *CEP290* alleles, would be predicted to produce no full-length or near-full-length CEP290 protein at all, contrary to what we discovered. Total CEP290 transcripts for each patient, as determined by quantitative polymerase chain reaction (PCR), were also found to correlate closely with expression predicted by our model (Fig. 4D).

To test whether nonsense-associated alternative splicing could account for the various amounts of CEP290 protein detected in our experiments, we sought to specifically detect alternatively spliced *CEP290* transcript in the complementary DNA (cDNA) of primary dermal fibroblasts from each of our patients and controls. We designed multiple PCR-based assays to amplify across the unique exon junctions that would occur only in *CEP290* transcripts skipping each particular exon mutated in our patients (Fig. 4A). For each exon that our model predicted to be skippable through the process of nonsense-associated alternative splicing, *CEP290* transcripts lacking that exon could be detected both in patients and, to our surprise, in normal controls (Fig. 4B). Such widespread basal exon skipping, occurring even in normal individuals and outside of the context of nonsense mutations, is an important and interesting finding and a plausible mechanistic explanation for the amounts of full-length and near-full-length CEP290 proteins we detected in our patient samples.

To more quantitatively analyze the degree of basal exon skipping in our different samples, we designed TaqMan PCR assays to specifically quantify *CEP290* transcripts lacking exon 6, 10, 41, or 46 in each of our patients and controls (Fig. 4C). Again, *CEP290* transcripts lacking each of the exons examined were detectable in every sample (Fig. 4D). In no patients did we find the amount of alternatively spliced transcript to be greater than that of alternatively spliced transcripts in controls, as the mechanism of nonsense-associated alternative splicing would require. Expression of each alternatively spliced transcript instead appeared to be directly related to total *CEP290* transcript, with a few exceptions (Fig. 4D), supporting the hypothesis that it is exon skipping, and not nonsense-induced alternative splicing, that contributes to the amounts of alternatively spliced message that we observed.

Our model of basal exon skipping, however, does imply that, in a patient with a truncating mutation in a particular exon, expression of *CEP290* transcripts lacking that exon should be relatively increased compared to that of total *CEP290* transcripts. Transcripts containing the mutated exon should be subject to nonsense-mediated decay, whereas those transcripts skipping the mutated exon should escape decay, making up a larger percent of total detectable *CEP290* transcript. For each exon examined, we normalized *CEP290* transcript lacking the exon in question to total *CEP290* transcript (Fig. 4D and fig. S2, A to C). Patient 582, harboring a truncating mutation in exon 41, was found to have a marked sixfold increase in *CEP290* transcript lacking exon 41, relative to total *CEP290* transcript, when compared to all other samples (Fig. 4D), providing direct evidence for the underlying mechanism of basal exon skipping. This relative increase in alternatively spliced transcript was not seen in our other patients with mutations in exons we would expect to be subject to basal exon skipping (fig. S2, A to C). However, unlike patient 582, each of these patients harbored at least one *CEP290* allele carrying the common c.1655A>G mutation, which results in high expression of normal *CEP290* transcript, potentially obscuring the relative increase in alternatively spliced transcripts that we would expect. Patient 582 was also found

to have increased expression of *CEP290* transcript lacking exon 46, suggesting that the alternative splicing of a specific exon may have more broadly reaching effects than our model had accounted for, and suggesting new ways to potentially improve our model.

To determine whether the implications of basal exon skipping and our model of pleiotropic disease extend beyond *CEP290* to other genes, we applied our model to the disease gene coiled-coil and C2 domain containing 2A (table S3), *CC2D2A*, which, similar to *CEP290*, is associated with MKS, JS, and JSRD (23–28). Unlike in *CEP290*, where more than 95% of JS patients manifest extra-CNS symptoms, most of *CC2D2A* patients diagnosed with JS have JS alone (that is, with no extra-CNS involvement). We separated the JS patients from patients with additional renal or retinal disease (JSRD) for our analysis. We found that CC2D2A protein expression, as predicted by our model, significantly correlated with disease severity ($P < 0.0001$, Fisher's exact test). One hundred percent of patients with JS were predicted to have medium to high amounts of CC2D2A. Patients with JSRD were found to have a more even distribution across different predicted protein amounts. Eighty percent of patients with MKS, on the other hand, were predicted to have very low or absent CC2D2A protein (Fig. 2D).

DISCUSSION

To date, the pleiotropic nature of *CEP290* disease has defied explanation despite scientific investigation and analysis. Here, we have presented data that accurately and robustly correlate *CEP290* mutations with clinical presentation and have described the mechanism by which these mutations result in predictable production of CEP290 protein and predictable disease phenotypes. Our model relies on the concepts of alternative splicing and exon skipping, phenomena that have recently been shown to occur with high frequency within the retina and other tissues (29) and which have been overlooked as a potential source of pleiotropy. We discovered that basal noncanonical exon skipping occurs both in patients with *CEP290* mutations and in normal controls, yielding abundant transcript variety and posing a potential solution to the problem of disease pleiotropy. Our data indicate that, in the face of premature stop mutations, basal exon skipping may provide nature with a potential workaround, supplying the cell with low levels of alternatively spliced transcripts lacking the mutated exon and potentially producing low amounts of near-full-length functional protein, resulting in predictable gradations of phenotypic severity.

Our study was limited in that we investigated only two genes, both implicated in the class of human disease syndromes known as ciliopathies. Additionally, we investigated transcript and protein levels in only a single tissue type, dermal fibroblasts. We cannot exclude the hypothesis that basal exon skipping may prove to be tissue-and gene-specific, relevant only to particular disease processes and organ systems. It must also be noted that the level of basal exon skipping occurring in the patient samples we tested was low. Preliminary experimentation using RNA-seq yielded no evidence of basal exon skipping, although the low number of reads through individual *CEP290* splice junctions may have obscured such infrequent alternative splicing events. Such low levels of basal exon skipping may only have meaningful implications for a small number of diseases in which a graded response to small increases in total protein can meaningfully affect the patient phenotype. With continued

investigation, it will be interesting to see whether this mechanism extends beyond the ciliopathies and ciliary disease genes to explain the genetics of pleiotropy and human disease more generally.

MATERIALS AND METHODS

Study design

Review of *CEP290* and *CC2D2A* genotype/phenotype relationships was carried out using published data (see below). Additional genotype/phenotype data were collected from patients seen at the retinal degeneration clinics at the Center for Advanced Retinal and Ocular Therapeutics and from the Stephen A. Wynn Institute for Vision Research. Genotyping was carried out at the John and Marcia Carver Nonprofit Genetic Testing Laboratory, University of Iowa. Tissue samples were also collected from patients seen at both centers using protocols approved by the respective Institutional Review Boards (IRBs). Molecular genetic testing of the samples was carried out to determine transcript and protein expression as described below. Results of molecular genetic testing were correlated with the predictions based on review of genotype/phenotype data.

Mutation analysis

Human mutations in *CEP290* were compiled from published articles and from the *CEP290* mutation database developed by F. Coppieters, S. Lefever, B. P. LeRoy, and E. De Baere at Ghent University and Ghent University Hospital, Ghent, Belgium (19). The coding effect of each mutation was noted, particularly with respect to whether an exon was predicted to be disrupted by a premature stop codon (because of either nonsense or frameshift mutations) or skipped because of a mutation affecting exon splicing. Mutations were then sorted into three groups. Mild mutations were those that were predicted to have little effect on total CEP290 protein levels (in-frame deletions, missense mutations, truncating mutations occurring within the last exon, and splicing mutations in which there is evidence for high levels of normal transcript production). Moderate mutations were those that were predicted to significantly reduce CEP290 protein levels (those that resulted in a premature stop codon within, or splicing mutation likely to result in the skipping of, an in-frame exon). Severe mutations were those that were predicted to act as null alleles (those that resulted in a premature stop codon within, or splicing mutation likely to result in the skipping of, an out-of-frame exon). The sorted mutations are listed in fig. S1. Mutations in the gene *CC2D2A* were sorted in an identical fashion. For our modified *CEP290* model, mutations affecting exon 6, 9, 40, or 41 were considered severe.

CEP290 mutant protein expression and disease phenotype prediction

A model for predicting the amount of full-length and near-full-length CEP290 proteins in patients for whom both *CEP290* disease alleles were known was devised as shown in Fig. 1B. The same model was applied to patients with mutations in CC2D2A.

Patient assessment

Patients were seen at the retinal degeneration clinics of the University of Iowa, Children's Hospital of Philadelphia, or Center for Advanced Retinal and Ocular Therapeutics

(University of Pennsylvania Perelman School of Medicine) where a family history was ascertained and the individuals received standard clinical examinations including assessments of visual acuity, visual fields, and retinal structure. The diagnosis of LCA was made by electroretinogram, and the diagnosis of JS was made by brain magnetic resonance imaging. Molecular genetic testing was carried out after obtaining IRB-approved consent/assent (plus parental permission).

Cells and cell culture

Primary dermal fibroblasts were isolated from patient skin punches after obtaining informed consent/assent, and these were grown in Dulbecco's modified Eagle's medium supplemented with 10% fetal bovine serum and 1% penicillin-streptomycin at 37°C in a humidified 5% CO_2 atmosphere. Fibroblasts were passaged fewer than 10 times before analysis.

CEP290 protein

Patient fibroblasts were washed with phosphate-buffered saline, and 5×10^6 cells were lysed by incubation in 50 μl of radioimmunoprecipitation assay buffer (50 mM tris, 150 mM NaCl, 0.1% SDS, 0.5% sodium deoxycholate, 1% Triton X-100) supplemented with a protease inhibitor cocktail for 30 min at 4°C. Cell lysates were centrifuged at 20,000*g* for 15 min to remove insoluble material, and the resulting supernatants were analyzed by SDS–polyacrylamide gel electrophoresis and immunoblotting using standard techniques. Blots were probed with antibodies against CEP290 (Abcam, ab105383) and α-tubulin (Abcam, ab7291) and imaged with a Typhoon 9400 instrument (GE).

cDNA isolation

cDNA was isolated from patient fibroblasts using Qiagen's RNeasy kit and Invitrogen's SuperScript III First-Strand Synthesis kit following the manufacturers' protocols.

Exon junction detection

Two primers plus a control forward primer were designed to amplify across the hypothetical exon junction of CEP290 transcripts lacking each exon examined, as in Fig. 4A, and used for PCR amplification of patient and control cDNAs. The resulting PCR products were resolved by agarose gel electrophoresis, imaged, gel-excised, and submitted for confirmatory Sanger sequencing. Primer sets for hypothetical exon junctions were as follows: exon 6, P_1: GAAAATGAACTGGAGTTGGCTCTTC, P_2: CACTGTCTTCCCCTCTTCTTG, and P_C: CTCTCTCTCTCT-CTTGGCTCTTC; exon 10, P_1: CTTGATGAAATTCAGGTG-CAGGAGC, P_2: CTGCTGTAGAGCCATAACATTAC, and P_C: CTCTCTCTCTCGTGCAGGAGC; exon 41, P_1: CCAGTGGAT-TACAGAATGCTAAAG, P_2: CCTGATCAACAGTCATGCCAG, and P_C: CTCTCTCTCTCTCTAATGCTAAAG; and exon 46, P_1: GATTTGCCAAGATTAAAGTCTGGTAG, P_2: GATTCATAGTG-CATGCTCAACTG, and P_C: CTCTCTCTCTCTCTTCTGGTAG.

TaqMan assay design and analysis

Custom TaqMan PCR assays were designed to specifically quantify levels of CEP290 transcript lacking particular exons as described in Fig. 4C. Additional TaqMan assays were carried out using commercially available kits for GAPDH and full-length CEP290 (Invitrogen). TaqMan assays were run using TaqMan Fast Universal Master Mix (Invitrogen), and all reactions were carried out on an Applied Biosys-tems 7500 Fast Real-Time PCR instrument. Relative quantification was accomplished with the $\Delta\Delta C_t$ method using Invitrogen's CloudSuite software.

Custom primer and probe sets were as follows: exon 6, primer 1: GAAGAACAAGCAAAATTTGAAAATC, primer 2: CGTTTGTTCTCT-CTTCTTAATTTGC, and probe: CGAAGAGCCAACTCCAGTTC-ATTTTCCA; exon 10, primer 1: ACAGTGACTACCGATCACAGTTGT, primer 2: CAAAATTAGCTTCCATTCTTCTACTTTT, and probe: AATATCTTGATGAAATTCAGGTGCAGGAGCTTAC; exon 41, primer 1: GATCAAGAGAATGATGAACTGAAAAG, primer 2: CTTGTTTCGAATTCCTTCTATTTTG, and probe: AAGACTAAC-CAGTGGATTACAGAATGCTAAAGAAGAATT; and exon 46, primer 1: GAAGGAAAACTTGAAGTTGTCATCTG, primer 2: TCAAC-TACTTTTTTCATTAAACCAATGG, and probe: TGTCTTTCCAC-TTCTACCAGACTTTAATCTTGGCA.

Statistical analysis

The statistical significance of the difference between three or more means was determined using a two-way ANOVA and Tukey's HSD (honestly significantly different) test. The statistical significance of the difference in predicted protein amounts across different phenotypes was determined using Fisher's exact test. Statistical analysis was performed using GraphPad Prism software 5.0b. *P* values <0.05 were considered significant.

Supplementary Material

Refer to Web version on PubMed Central for supplementary material.

Acknowledgments

We thank the *CEP290* patients and their families who made this work possible through the donation of their samples and time.

Funding: Supported by Project CEP290 and the Grousbeck Family Foundation. Additional support was provided by the Foundation Fighting Blindness; Research to Prevent Blindness; NIH R24EY019861, 1F30AG044078-01A1, 1R24 EY019861-01A1, 8DP1EY023177, and 1DP2OD007483; Howard Hughes Medical Institute; Treatrush (European Union); Transdisciplinary Awards Program in Translational Medicine and Therapeutics (University of Pennsylvania); the Mackall Foundation Trust; the Pennsylvania Department of Health (Penn Genome Frontiers Institute); and the F.M. Kirby Foundation.

REFERENCES AND NOTES

1. Solovieff N, Cotsapas C, Lee PH, Purcell SM, Smoller JW. Pleiotropy in complex traits: Challenges and strategies. Nat Rev Genet. 2013; 14:483–495. [PubMed: 23752797]

2. Vuoristo MM, Pappas JG, Jansen V, Ala-Kokko L. A stop codon mutation in COL11A2 induces exon skipping and leads to non-ocular Stickler syndrome. Am J Med Genet A. 2004; 130A:160–164. [PubMed: 15372529]

3. Chang Y-F, Chan W-K, Imam JS, Wilkinson MF. Alternatively spliced T-cell receptor transcripts are up-regulated in response to disruption of either splicing elements or reading frame. J Biol Chem. 2007; 282:29738–29747. [PubMed: 17693403]

4. Puisac B, Teresa-Rodrigo ME, Arnedo M, Gil-Rodríguez MC, Pérez-Cerdá C, Ribes A, Pié A, Bueno G, Gómez-Puertas P, Pié J. Analysis of aberrant splicing and nonsense-mediated decay of the stop codon mutations c.109G>T and c.504_505delCT in 7 patients with HMG-CoA lyase deficiency. Mol Genet Metab. 2013; 108:232–240. [PubMed: 23465862]

5. Wang J, Chang YF, Hamilton JI, Wilkinson MF. Nonsense-associated altered splicing: A frame-dependent response distinct from nonsense-mediated decay. Mol Cell. 2002; 10:951–957. [PubMed: 12419238]

6. Littink KW, Pott JW, Collin RW, Kroes HY, Verheij JB, Blokland EA, de Castro Miró M, Hoyng CB, Klaver CC, Koenekoop RK, Rohrschneider K, Cremers FP, van den Born LI, den Hollander AI. A novel nonsense mutation in *CEP290* induces exon skipping and leads to a relatively mild retinal phenotype. Invest Ophthalmol Vis Sci. 2010; 51:3646–3652. [PubMed: 20130272]

7. Perrault I, Delphin N, Hanein S, Gerber S, Dufier JL, Roche O, Defoort-Dhellemmes S, Dollfus H, Fazzi E, Munnich A, Kaplan J, Rozet JM. Spectrum of NPHP6/CEP290 mutations in Leber congenital amaurosis and delineation of the associated phenotype. Hum Mutat. 2007; 28:416. [PubMed: 17345604]

8. Drivas TG, Bennett J. CEP290 and the primary cilium. Adv Exp Med Biol. 2014; 801:519–525. [PubMed: 24664739]

9. D'Angelo A, Franco B. The dynamic cilium in human diseases. PathoGenetics. 2009; 2:3. [PubMed: 19439065]

10. Drivas TG, Holzbaur ELF, Bennett J. Disruption of CEP290 microtubule/membrane-binding domains causes retinal degeneration. J Clin Invest. 2013; 123:4525–4539. [PubMed: 24051377]

11. Davenport JR, Watts AJ, Roper VC, Croyle MJ, van Groen T, Wyss JM, Nagy TR, Kesterson RA, Yoder BK. Disruption of intraflagellar transport in adult mice leads to obesity and slow-onset cystic kidney disease. Curr Biol. 2007; 17:1586–1594. [PubMed: 17825558]

12. Han YG, Kim HJ, Dlugosz AA, Ellison DW, Gilbertson RJ, Alvarez-Buylla A. Dual and opposing roles of primary cilia in medulloblastoma development. Nat Med. 2009; 15:1062–1065. [PubMed: 19701203]

13. Wong SY, Seol AD, So PL, Ermilov AN, Bichakjian CK, Epstein EH Jr, Dlugosz AA, Reiter JF. Primary cilia can both mediate and suppress Hedgehog pathway–dependent tumorigenesis. Nat Med. 2009; 15:1055–1061. [PubMed: 19701205]

14. Papon JF, Perrault I, Coste A, Louis B, Gérard X, Hanein S, Fares-Taie L, Gerber S, Defoort-Dhellemmes S, Vojtek AM, Kaplan J, Rozet JM, Escudier E. Abnormal respiratory cilia in non-syndromic Leber congenital amaurosis with *CEP290* mutations. J Med Genet. 2010; 47:829–834. [PubMed: 20805370]

15. Halbritter J, Diaz K, Chaki M, Porath JD, Tarrier B, Fu C, Innis JL, Allen SJ, Lyons RH, Stefanidis CJ, Omran H, Soliman NA, Otto EA. High-throughput mutation analysis in patients with a nephronophthisis-associated ciliopathy applying multiplexed barcoded array-based PCR amplification and next-generation sequencing. J Med Genet. 2012; 49:756–767. [PubMed: 23188109]

16. Otto EA, Ramaswami G, Janssen S, Chaki M, Allen SJ, Zhou W, Airik R, Hurd TW, Ghosh AK, Wolf MT, Hoppe B, Neuhaus TJ, Bockenhauer D, Milford DV, Soliman NA, Antignac C, Saunier S, Johnson CA, Hildebrandt F. GPN Study Group. Mutation analysis of 18 nephronophthisis associated ciliopathy disease genes using a DNA pooling and next generation sequencing strategy. J Med Genet. 2011; 48:105–116. [PubMed: 21068128]

17. Yzer S, Hollander AI, Lopez I, Pott JW, de Faber JT, Cremers FP, Koenekoop RK, van den Born LI. Ocular and extra-ocular features of patients with Leber congenital amaurosis and mutations in *CEP290*. Mol Vis. 2012; 18:412–425. [PubMed: 22355252]

18. Wiszniewski W, Lewis RA, Stockton DW, Peng J, Mardon G, Chen R, Lupski JR. Potential involvement of more than one locus in trait manifestation for individuals with Leber congenital amaurosis. Hum Genet. 2011; 129:319–327. [PubMed: 21153841]

19. Coppieters F, Lefever S, Leroy BP, De Baere E. *CEP290*, a gene with many faces: Mutation overview and presentation of CEP290*base*. Hum Mutat. 2010; 31:1097–1108. [PubMed: 20690115]

20. den Hollander AI, Koenekoop RK, Yzer S, Lopez I, Arends ML, Voesenek KE, Zonneveld MN, Strom TM, Meitinger T, Brunner HG, Hoyng CB, van den Born LI, Rohrschneider K, Cremers FP. Mutations in the *CEP290* (*NPHP6*) gene are a frequent cause of Leber congenital amaurosis. Am J Hum Genet. 2006; 79:556–561. [PubMed: 16909394]

21. Maquat LE. Nonsense-mediated mRNA decay: Splicing, translation and mRNP dynamics. Nat Rev Mol Cell Biol. 2004; 5:89–99. [PubMed: 15040442]

22. Baker KE, Parker R. Nonsense-mediated mRNA decay: Terminating erroneous gene expression. Curr Opin Cell Biol. 2004; 16:293–299. [PubMed: 15145354]

23. Gorden NT, Arts HH, Parisi MA, Coene KL, Letteboer SJ, van Beersum SE, Mans DA, Hikida A, Eckert M, Knutzen D, Alswaid AF, Ozyurek H, Dibooglu S, Otto EA, Liu Y, Davis EE, Hutter CM, Bammler TK, Farin FM, Dorschner M, Topçu M, Zackai EH, Rosenthal P, Owens KN, Katsanis N, Vincent JB, Hildebrandt F, Rubel EW, Raible DW, Knoers NV, Chance PF, Roepman R, Moens CB, Glass IA, Doherty D. *CC2D2A* is mutated in Joubert syndrome and interacts with the ciliopathy-associated basal body protein CEP290. Am J Hum Genet. 2008; 83:559–571. [PubMed: 18950740]

24. Mougou-Zerelli S, Thomas S, Szenker E, Audollent S, Elkhartoufi N, Babarit C, Romano S, Salomon R, Amiel J, Esculpavit C, Gonzales M, Escudier E, Leheup B, Loget P, Odent S, Roume J, Gérard M, Delezoide AL, Khung S, Patrier S, Cordier MP, Bouvier R, Martinovic J, Gubler MC, Boddaert N, Munnich A, Encha-Razavi F, Valente EM, Saad A, Saunier S, Vekemans M, Attié-Bitach T. *CC2D2A* mutations in Meckel and Joubert syndromes indicate a genotype-phenotype correlation. Hum Mutat. 2009; 30:1574–1582. [PubMed: 19777577]

25. Noor A, Windpassinger C, Patel M, Stachowiak B, Mikhailov A, Azam M, Irfan M, Siddiqui ZK, Naeem F, Paterson AD, Lutfullah M, Vincent JB, Ayub M. *CC2D2A*, encoding a coiled-coil and C2 domain protein, causes autosomal-recessive mental retardation with retinitis pigmentosa. Am J Hum Genet. 2008; 82:1011–1018. [PubMed: 18387594]

26. Tallila J, Jakkula E, Peltonen L, Salonen R, Kestilä M. Identification of *CC2D2A* as a Meckel syndrome gene adds an important piece to the ciliopathy puzzle. Am J Hum Genet. 2008; 82:1361–1367. [PubMed: 18513680]

27. Bachmann-Gagescu R, Ishak GE, Dempsey JC, Adkins J, O'Day D, Phelps IG, Gunay-Aygun M, Kline AD, Szczaluba K, Martorell L, Alswaid A, Alrasheed S, Pai S, Izatt L, Ronan A, Parisi MA, Mefford H, Glass I, Doherty D. Genotype–phenotype correlation in *CC2D2A*-related Joubert syndrome reveals an association with ventriculomegaly and seizures. J Med Genet. 2012; 49:126–137. [PubMed: 22241855]

28. Szymanska K, Berry I, Logan CV, Cousins SR, Lindsay H, Jafri H, Raashid Y, Malik-Sharif S, Castle B, Ahmed M, Bennett C, Carlton R, Johnson CA. Founder mutations and genotype-phenotype correlations in Meckel-Gruber syndrome and associated ciliopathies. Cilia. 2012; 1:18. [PubMed: 23351400]

29. Farkas MH, Grant GR, White JA, Sousa ME, Consugar MB, Pierce EA. Transcriptome analyses of the human retina identify unprecedented transcript diversity and 3.5 Mb of novel transcribed sequence via significant alternative splicing and novel genes. BMC Genomics. 2013; 14:486. [PubMed: 23865674]

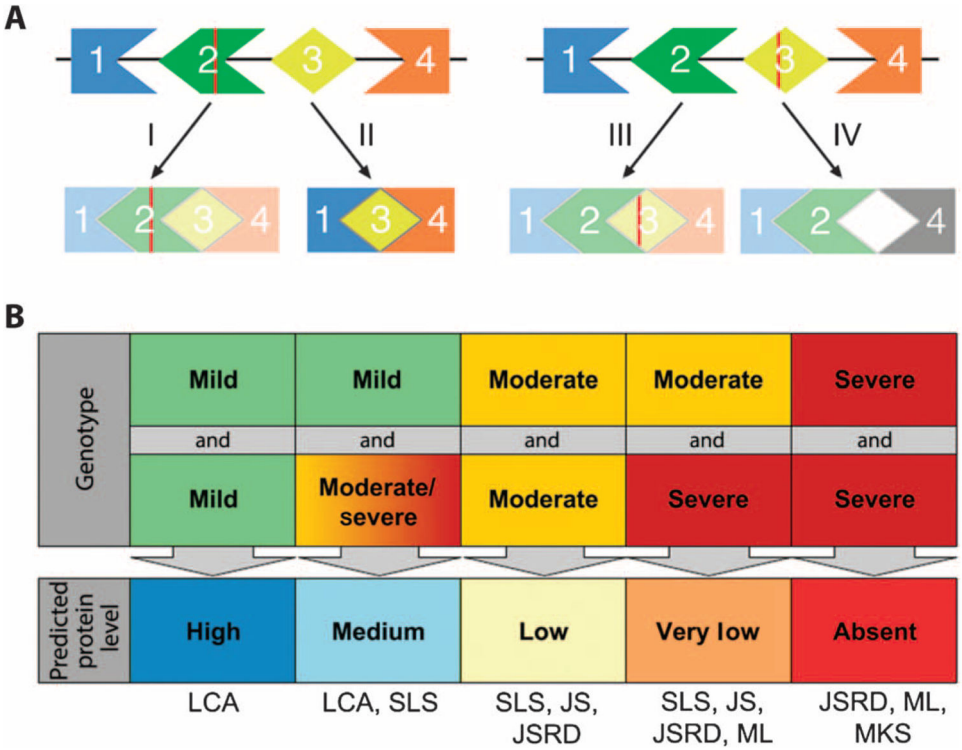

Fig. 1. A model to explain the pleiotropy of CEP290 disease

(**A**) A schematic of nonsense-induced alternative splicing. (I and III) A gene transcript containing a nonsense mutation (red line) undergoes canonical splicing. In both cases, the inclusion of the exon harboring the nonsense mutation targets the transcript for nonsense-mediated decay. (II) Alternative splicing yields a transcript lacking exon 2 and the premature stop codon. The message persists and results in a truncated but otherwise intact open reading frame. (IV) Alternative splicing yields a transcript lacking exon 3 and the premature stop codon but containing a frameshift from the splicing together of incompatible exon ends, resulting in nonsense-mediated decay. (**B**) A model for predicting CEP290 protein production in individual patients for whom both *CEP290* disease alleles are known (fig. S1). Listed below the model are the CEP290 disease phenotypes predicted to be associated with each protein amount.

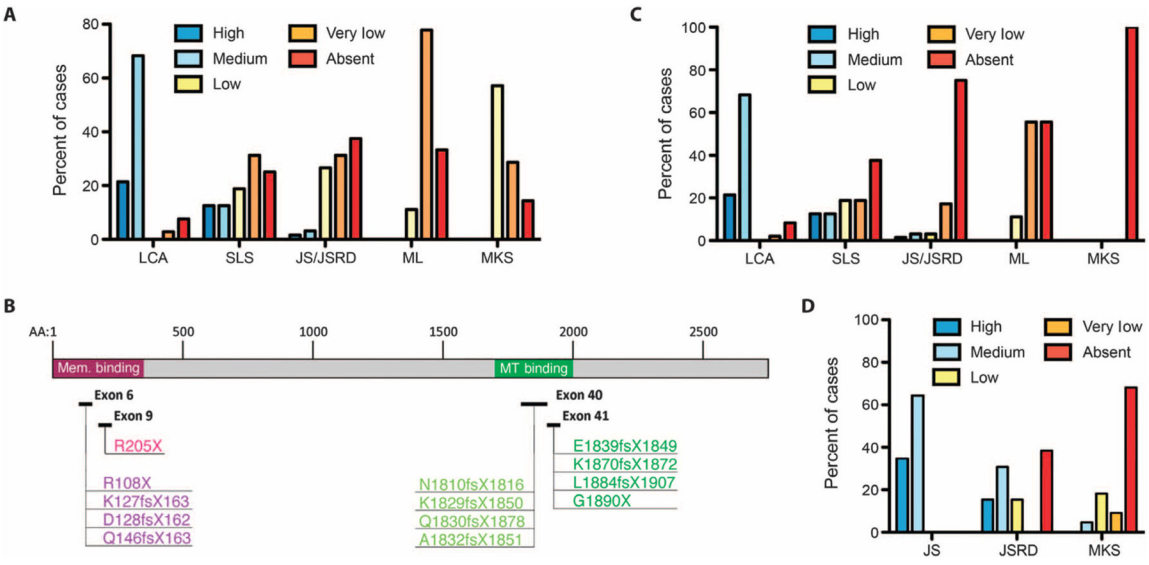

Fig. 2. Predicted CEP290 prote`in expression correlates with patient phenotype

(**A**) Predicted CEP290 protein is plotted as a percent of total cases for each phenotype. LCA, *n* = 145; SLS, *n* = 16; JS/JSRD, *n* = 64; ML, *n* = 9; and MKS, *n* = 14. Predicted protein expression correlates with disease severity ($P < 0.0001$, Fisher's exact test). (**B**) Scale representation of CEP290 indicating the location of mutations in exons 6, 9, 40, and 41 in relation to the protein's membrane (Mem.)– and microtubule (MT)–binding domains. (**C**) Predicted expression of CEP290 protein with intact membrane-binding and microtubule-binding domains was determined as described in the text. Annotations and patient numbers are as in (A). Predicted protein production was associated with disease severity ($P < 0.0001$, Fisher's exact test). (**D**) Predicted CC2D2A protein production was plotted as a percent of total cases for each phenotype. JS, including patients with only CNS disease, *n* = 23; JSRDs, including patients with JS with additional extra-CNS manifestations, *n* = 14; and MKS, *n* = 15. Predicted protein production was associated with disease severity ($P < 0.0001$, Fisher's exact test).

A

Patient	Age (yrs)	Gender	Nucleotide alteration	Coding effect	Predicted protein level	Ocular symptoms	CNS symptoms	Renal symptoms	Diagnosis
54	9	F	IVS26 + 1655 A>G IVS26 + 1655 A>G	Cryptic exon Cryptic exon	High	VF	NOD	NOD	LCA
62	23	M	IVS26 + 1655 A>G Val247 739delG	Cryptic exon Exon 10 FS	Medium	VFNA	NOD	NOD	LCA
182	7	F	IVS26 + 1655 A>G Lys127 379delA 380delA	Cryptic exon Exon 6 FS	Medium	NLP	ID	NOD	LCA
294	14	M	IVS26 + 1655 A>G Thr835 2503delA 2504delC	Cryptic exon Exon 24 FS	Medium	NLP	NOD	NOD	LCA
582	19	M	Arg549Stop 1645 C>T Lys1882 5643_5644 insA	Exon 17 S Exon 41 FS	Very low	VFNA	JS	NOD	JSRD
619	5	M	IVS26 + 1655 A>G Val2093 6277delG	Cryptic exon Exon 46 FS	Medium	VFNA	NOD	NOD	LCA
620	4	M	IVS26 + 1655 A>G Val2093 6277delG	Cryptic exon Exon 46 FS	Medium	VFNA	NOD	NOD	LCA

FS, frameshift; S, premature stop codon; VF, measurable visual fields; VFNA, visual fields not able to be measured, light perception only; NLP, no light perception; ID, intellectual disability; NOD, no overt disease.

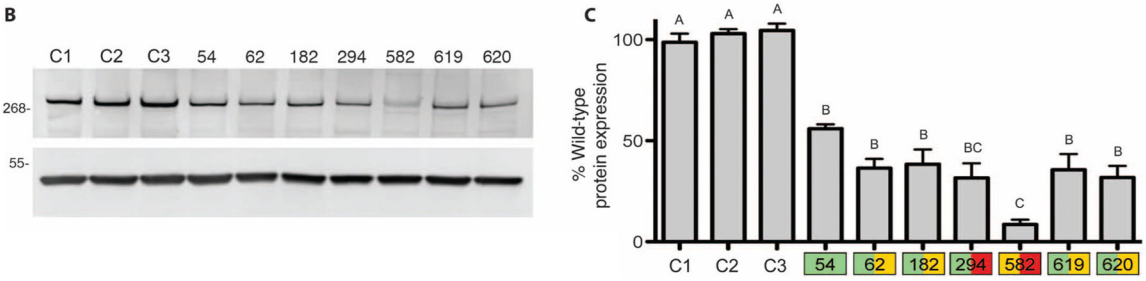

Fig. 3. Predicted CEP290 protein production correlates with actual CEP290 protein expression

(**A**) Clinical features, mutations, and predicted protein expression for seven patients with *CEP290* mutations. Color coding is as in Fig. 1B. Boxes with orange and red stripes indicate mutations expected to produce low levels of CEP290 lacking the critical exon 6 or 41. (**B**) Immunoblot of fibroblast lysates from seven patients with *CEP290* mutations (numbered) and three normal controls (C1, C2, and C3) probed for CEP290 (top) and α-tubulin as a loading control (bottom). Molecular masses are indicated in kilodaltons. (**C**) Den-sitometric analysis of CEP290 protein expression as in (B). Exact values are shown in table S4. Data are presented as means ± SD ($n = 4$). Means with different letters are significantly different; $P < 0.05$, determined by analysis of variance (ANOVA).

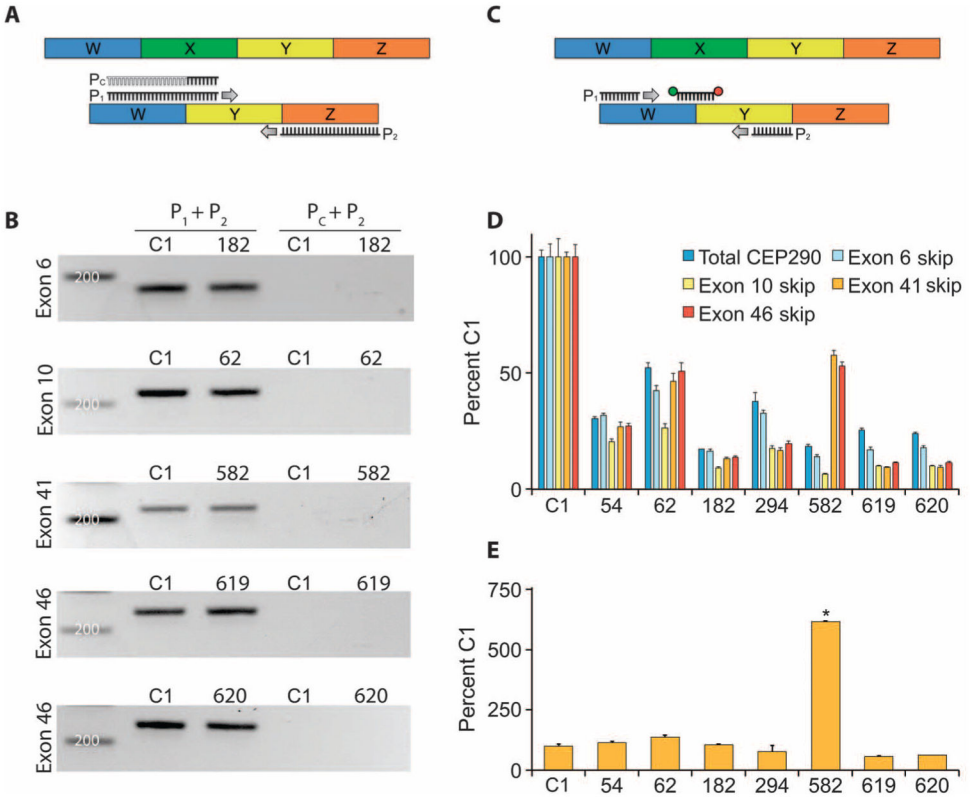

Fig. 4. Basal skipping of *CEP290* exons 6, 10, 41, and 46 occurs in all samples tested

(**A**) A PCR primer (P_1) was designed to anneal only to the hypothetical exon W–exon Y junction created by the omission of exon X. A similar primer (P_C), substituting a random sequence of bases for the exon W–complementary region, was designed to serve as a negative control. PCR amplification was carried out under identical conditions using each of these two primers and a reverse primer (P_2) located in a downstream exon. The presence of PCR products in only the $P_1 + P_2$ reaction indicates the presence of *CEP290* transcript lacking exon X. (**B**) Agarose gels showing PCR products obtained from patient (numbered) and normal control (C1) fibroblast cDNA. Experimental ($P_1 + P_2$, lanes 2 and 3) and control ($P_C + P_2$, lanes 4 and 5) PCRs were carried out as in (A). For each exon examined, alternatively spliced *CEP290* transcript skipping the exon in question was clearly detected in both patients and controls. Relevant DNA ladder bands are indicated (unlabeled lane 1). (**C**) TaqMan PCR assays were designed with a probe that would anneal specifically to the exon W–exon Y junction created by the omission of exon X, with appropriate upstream and downstream primers. (**D**) Total *CEP290* transcript and *CEP290* transcript lacking exon 6, 10, 41, or 46 in patient (numbered) and normal control (C1) fibroblast cDNA as determined by TaqMan PCR as in (C). Relative expression was determined using the $\Delta\Delta C_t$ method normalizing to GAPDH (glyceraldehyde phosphate dehydrogenase) and adjusting all *CEP290* transcript species to percent of normal control C1. Data are presented as means ± SD ($n = 3$). (**E**) *CEP290* transcript lacking exon 41 in patient (numbered) and normal control (C1) fibroblast cDNA as determined by TaqMan PCR. Data were normalized to total *CEP290* transcript and adjusted to percent of normal C1 using the $\Delta\Delta C_t$ method. Data are

presented as means ± SD (n = 3); means marked with an asterisk are significantly different from all other means, with $P < 0.0001$. (D and E) Exact values are shown in table S4.